

Contract No.:

This manuscript has been authored by Savannah River Nuclear Solutions (SRNS), LLC under Contract No. DE-AC09-08SR22470 with the U.S. Department of Energy (DOE) Office of Environmental Management (EM).

Disclaimer:

The United States Government retains and the publisher, by accepting this article for publication, acknowledges that the United States Government retains a non-exclusive, paid-up, irrevocable, worldwide license to publish or reproduce the published form of this work, or allow others to do so, for United States Government purposes.

Spectroscopy of Palladium Nanoparticle Synthesis: Tailoring Nanoparticle Growth Parameters for Hydrogen Storage

Amanda L. Houk^{1*} and Levi R. Houk^{1*}

¹Savannah River National Laboratory, Aiken, SC 29808, U.S.A.

*Corresponding Authors: amanda.houk@srnl.doe.gov, levi.houk@srnl.doe.gov

ABSTRACT

Using palladium for hydrogen storage requires palladium (Pd) particles exhibiting specific parameters, including surface area, particle size, and particle shape, with increased interest in palladium nanoparticles (Pd NPs). In order to routinely monitor the synthesis of these particles a spectroscopic method is being developed using infrared (IR), Raman, and UV-Vis spectroscopy. By monitoring the production of Pd NPs, the growth of the NPs can be controlled to ensure quality of the product to match the desired finished particle specifications. For the reaction presented, the conversion of the intermediate tetraamminepalladium(II) chloride (PTC) to diamminepalladium(II) chloride (PDC) can influence the Pd NPs properties. This study is first being developed in lab bench scale quantities to allow ultimate control of the Pd NPs.

INTRODUCTION

Using palladium (Pd) as a hydrogen storage material has been prevalent in the literature as early as the 1960s [1] because of the novel way hydrogen is stored in the Pd metal lattice. Currently there is more of an emphasis on Pd hydride systems as it pertains to potential advances in the hydrogen economy [2]. In recent years, a wide variety of shapes [3-5] and sizes [6, 7] have been studied for improved Pd hydride systems. As these complicated Pd nanostructures see more interest in the academic setting, industrial

implications where quality and control of the size and structure of a potential product must be realized. A greater ability to control the synthesis of these reactions is needed to create Pd nanoparticles (NPs) within constraints of a defined product definition.

At the Savannah River Site (SRS), hydrogen and its isotopes are stored on Pd beds. The Pd NPs of interest in this study, which are produced in large, industrial quantities for SRS, are synthesized by the reaction of $\text{Pd}(\text{NH}_3)_4\text{Cl}_2$, tetraamminepalladium(II) chloride (PTC) with formic acid. During this reaction, Pd NPs are formed as nano-nodules, as these nano-nodules grow, they coalesce with other nano-nodules forming large linking chains of micro-clusters (Figure 1).

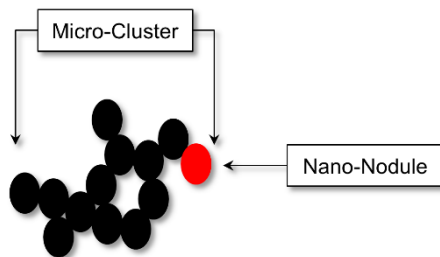


Figure 1. Illustration of how nano-nodules form micro-clusters.

Depending on the reaction conditions, even small changes in pH, reactant concentration/amounts, can have large impacts on the size and shape of the nano-nodule. Even under similar reaction conditions, the morphology and composition of the nano-nodules can vary [8]. We expect by monitoring key steps in the reaction with spectroscopy (infrared (IR), Raman, and UV-Vis) that these synthesis variations can be eliminated. The research presented here is a qualitative initial approach to understand the reaction from PTC to $\text{Pd}(\text{NH}_3)_2\text{Cl}_2$, diamminepalladium(II) chloride (PDC) and ultimately to Pd NPs in future work.

EXPERIMENTAL DETAILS

Sample preparation

One step in the synthesis of Pd NPs is to purify an intermediate, PTC. An unpurified-PTC (u-PTC) is synthesized by reacting ammonium hydroxide with palladium chloride (Figure 2(a)). The u-PTC is then reacted with acetic acid to remove two ammine groups from the u-PTC, creating a precipitated $\text{Pd}(\text{NH}_3)_2\text{Cl}_2$, or PDC (Figure 2(b)). PDC is then washed three times with deionized (DI) water (Figure 2(c-e)). The final step for purification is to create a purified-PTC (p-PTC) by reacting the third washing of PDC with ammonium hydroxide (Figure 2(f)). All samples are saturated to drive the reaction forward and to increase signal for the spectroscopy measurements.

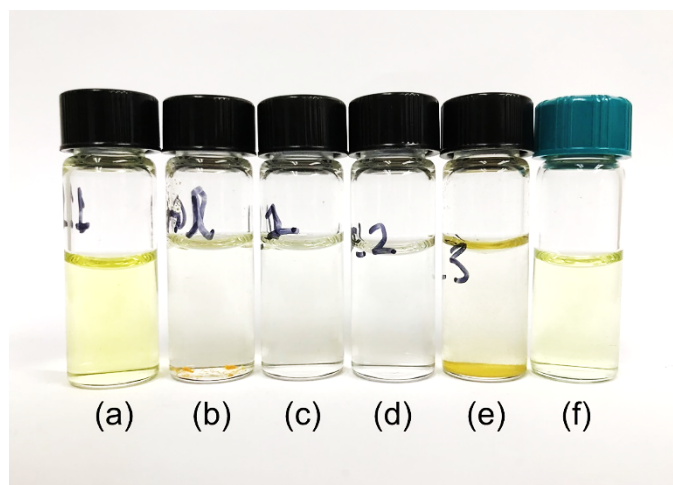


Figure 2. Image of samples in glass vials of (a) u-PTC, (b) PDC, (c) wash 1, (d) wash 2, (e) wash 3, and (f) p-PTC.

FTIR-ATR spectroscopy

Fourier Transform Infrared Reflectance (FTIR) spectra were collected with a Nicolet 7600 FTIR Spectrometer (Thermo Electron Corp.). An attenuated total reflectance (ATR) accessory with a diamond crystal at a 45° angle of incidence was used to measure the FTIR-ATR spectra. Spectra were collected from 4000 to 1000 cm^{-1} with a DTGS KBr detector. A resolution of 4 cm^{-1} was used to collect the spectra and 128 scans were averaged to obtain the final spectra.

Raman spectroscopy

Raman spectra were collected with a portable i-Raman Pro spectrometer (BWS475-785H-HT, Metrohm). The excitation wavelength used was 785 nm with about 320 mW of laser power. The spectral range of the spectrometer was 65 to 2800 cm^{-1} . Spectra were collected in 2-5 seconds. The samples were in glass vials (Figure 2) and spectra were measured through the vials with the attached fiber optic Raman probe.

UV-Vis spectroscopy

UV-Vis spectra were collected with a Lambda 45 UV-Vis spectrometer (PerkinElmer). Samples were placed in plastic cuvettes with a pathlength of 4 mm. Spectra were measured from 235 to 650 nm with a resolution of 1 nm.

DISCUSSION

FTIR-ATR spectroscopy

Figure 3 shows FTIR-ATR spectra of the conversion of u-PTC to p-PTC. The FTIR-ATR spectrum of u-PTC in Figure 3(a) has three distinct vibrational bands peaked near 3270, 1631, and 1306 cm^{-1} , which match literature values [9-13]. These bands are all

attributed to the ammine group in the u-PTC complex. Two vibrational modes contribute to the broad band peaked near 3270 cm^{-1} , the symmetric and asymmetric stretching modes of NH_3 [9-13]. The symmetric and asymmetric bending modes of NH_3 are the bands at 1306 and 1631 cm^{-1} , respectively [9-13]. After adding acetic acid to the u-PTC solution PDC slowly starts to form as shown in Figure 3(b). The conversion is shown by the bands near 3270 cm^{-1} separating and peaking near 3338 and 3224 cm^{-1} and the red-shifting of the symmetric bending mode to 1281 cm^{-1} . The shoulder bands near 3047 and 2865 cm^{-1} and the bands near 1550 and 1415 cm^{-1} are from excess acetic acid in solution. The excess acetic acid is completely removed following the three DI water washes, as shown in Figure 3(e). The vibrational bands for PDC following the three DI water washes are located near 3329 , 3255 , and 1635 cm^{-1} , which are the NH_3 asymmetric stretching, symmetric stretching, and asymmetric bending modes, respectively [13-15]. Ammonium hydroxide is added to PDC (Figure 3(e)) and converted to p-PTC (Figure 3(f)). The vibrational bands in p-PTC are identical to u-PTC.

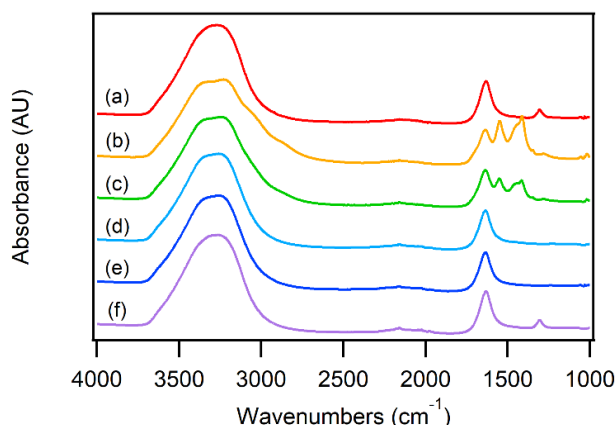


Figure 3. FTIR-ATR spectra of (a) u-PTC, (b) PDC, (c) wash 1, (d) wash 2, (e) wash 3, and (f) p-PTC.

Raman spectroscopy

Figure 4 shows Raman spectra of the conversion of u-PTC to p-PTC. The Raman spectrum of u-PTC in Figure 4(a) has three bands attributed to vibrational motions involving Pd. These bands are located near 268 , 470 , and 502 cm^{-1} , which are the bending N-Pd-N, asymmetric stretching Pd-N, and symmetric Pd-N modes, respectively [9, 11, 13]. The bands in the 1250 - 1650 cm^{-1} range are attributed to ammine vibrational modes [9-13]. The bands ranging from 1287 - 1333 cm^{-1} are symmetric stretching H-N-H modes and the bands from 1520 - 1637 cm^{-1} are asymmetric stretching H-N-H modes [9-13]. The low intensity, broad band near 796 cm^{-1} is likely related to the rocking motion of NH_3 [9-11, 13]. Acetic acid is added to the u-PTC solution, which slowly starts to form PDC as shown in Figure 4(b). This transition from u-PTC to PDC is shown by the band at 502 cm^{-1} red-shifting to 493 cm^{-1} . The bands near 650 , 930 , 1350 , and 1415 cm^{-1} are from excess acetic acid in solution. Excess acetic acid is completely removed following three DI water washes (Figure 4(e)). PDC is clearly observed after wash 3 in Figure 4(e), evidenced by the bands at 222 , 294 , and 493 cm^{-1} [13, 15]. The additional vibrational bands ranging from 1287 - 1333 cm^{-1} and 1520 - 1637 cm^{-1} are the symmetric stretching H-N-H modes and the asymmetric stretching H-N-H modes, respectively [9, 13-15]. Ammonium hydroxide

is added to PDC and is converted to p-PTC (Figure 4(f)). The majority of the vibrational bands in p-PTC are identical to u-PTC, Figure 4(a). The only difference is the addition of a band near 1400 cm^{-1} in the p-PTC spectrum, which may be attributed to another symmetric stretching H-N-H mode [11].

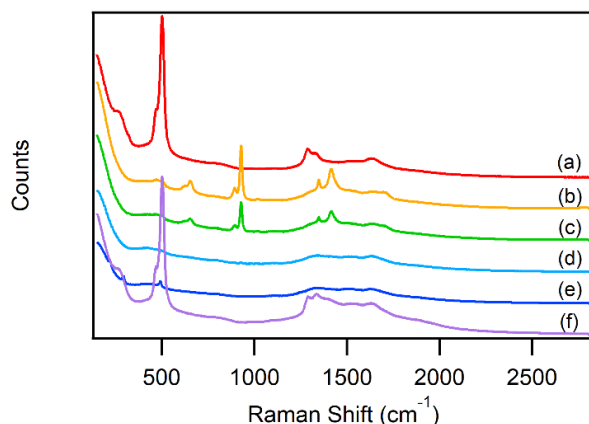


Figure 4. Raman spectra of (a) u-PTC, (b) PDC, (c) wash 1, (d) wash 2, (e) wash 3, and (f) p-PTC.

UV-Vis spectroscopy

Figure 5 shows UV-Vis spectra of the conversion of u-PTC to p-PTC. The absorbance spectra show that the band near 300 nm (4.13 eV) decreases in intensity and red-shifts to 350 nm (3.54 eV) after adding acetic acid to u-PTC (Figure 5(a)) to form PDC following three washes with DI water (Figure 5(b-e)). When ammonium hydroxide is added to Figure 5(e) the solution is converted to p-PTC (Figure 5(f)). UV-Vis spectra allow band gaps of materials to be calculated, specifically calculating the energy gap between the highest occupied molecular orbitals (HOMO) and lowest unoccupied molecular orbitals (LUMO) of materials. The lower energy band gaps for all solutions were 2.00 eV. The higher energy band gaps for u-PTC and p-PTC were similar, which were 2.68 and 2.76 eV, respectively. For PDC the higher energy band gap was 2.89 eV and decreased after each DI water wash to 2.82, 2.47, and 1.77 eV, respectively.

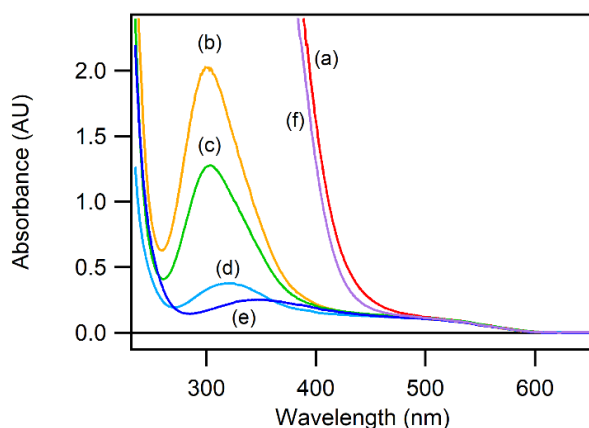


Figure 5. UV-Vis spectra of (a) u-PTC, (b) PDC, (c) wash 1, (d) wash 2, (e) wash 3, and (f) p-PTC.

CONCLUSIONS

We have demonstrated the ability to spectroscopically differentiate the different reaction intermediates that are needed to synthesize Pd NPs. IR, Raman, and UV-Vis spectroscopy distinctly showed differences for each step of the reaction from u-PTC to PDC to p-PTC. The spectra of u-PTC and p-PTC were almost identical for all three spectroscopy methods. The clearest spectra of PDC were measured after the third wash with DI water, after removing the excess acetic acid from the solution. All of this spectral information will be used for future studies of the reaction to form Pd NPs.

ACKNOWLEDGEMENTS

This work was funded by the Laboratory Directed Research & Development program at Savannah River National Laboratory under project number LDRD-2020-00050. This manuscript was authored by Savannah River Nuclear Solutions, LLC under Contract No. DE-AC09-08SR22470 with the U.S. Department of Energy. The United States Government retains and the publisher, by accepting this article for publication, acknowledges that the United States Government retains a non-exclusive, paid-up, irrevocable, worldwide license to publish or reproduce the published form of this work, or allow others to do so, for United States Government purposes.

REFERENCES

1. F. A. Lewis, *Platinum Metals Rev.* **26** (1), 20 (1982).
2. B. D. Adams and A. Chen, *Mater. Today* **14** (6), 282 (2011).
3. H. Huang, S. Bao, Q. Chen, Y. Yang, Z. Jiang, Q. Kuang, X. Wu, Z. Xie and L. Zheng, *Nano Res.* **8** (8), 2698 (2015).
4. F. J. Valencia, R. I. González, D. Tramontina, J. Rogan, J. A. Valdivia, M. Kiwi and E. M. Bringa, *J. Phys. Chem. C* **120** (41), 23836 (2016).
5. S. Kishore, J. A. Nelson, J. H. Adair and P. C. Eklund, *J. Alloys Compd.* **389** (1), 234 (2005).

6. M. Yamauchi, R. Ikeda, H. Kitagawa and M. Takata, *J. Phys. Chem. C* **112** (9), 3294 (2008).
7. S. K. Konda and A. Chen, *Mater. Today* **19** (2), 100 (2016).
8. D. P. Baldwin, D. S. Zamzow, R. D. Vigil and J. T. Piktuna, Report No. IS-5149, 2001.
9. C. H. Perry, D. P. Athans, E. F. Young, J. R. Durig and B. R. Mitchell, *Spectrochim. Acta A* **23** (4), 1137 (1967).
10. K. H. Schmidt and A. Müller, *J. Mol. Struct.* **22** (3), 343 (1974).
11. M. Manfait, A. J. P. Alix and J. Delaunay-Zeches, *Inorg. Chim. Acta* **44** L261 (1980).
12. Y.-J. Oh, S. M. Cho and C.-H. Chung, *J. Electrochem. Soc.* **152** (6), C348 (2005).
13. K. Nakamoto, *Infrared and Raman Spectra of Inorganic and Coordination Compounds: Part B: Applications in Coordination, Organometallic, and Bioinorganic Chemistry*, 6th ed. (John Wiley & Sons, Inc., Hoboken, New Jersey, 2008) p. 409.
14. R. Layton, D. W. Sink and J. R. Durig, *J. Inorg. Nucl. Chem.* **28** (9), 1965 (1966).
15. S. M. Fiuza, A. M. Amado, H. F. D. Santos, M. P. M. Marques and L. A. E. B. d. Carvalho, *Phys. Chem. Chem. Phys.* **12** (42), 14309 (2010).